Title

Evaluation of demolding force for glass-imprint process

Hiroshi Ikeda[1], Haruya Kasa[1], Hiroaki Nishiyama[1], Junji Nishii[1*].

Affiliation: [1] Research Institute for Electronic Science, Hokkaido University.

Address; N20 W10, Kita-ku, Sapporo, Hokkaido 001-0020, Japan.

Corresponding author:

*Junji.Nishii,

E-mail; nishii@es.hokudai.ac.jp

Tel & Fax; +81(11)-706-9377

Address; N20 W10, Kita-ku, Sapporo, Hokkaido 001-0020, Japan.

Abstract

Demolding behavior of oxide glasses from molds was experimentally analyzed using a specially developed molding set up equipped with highly sensitive load cell and servomotor. The demolding point and the demolding force were apt to increase with the tensile force applied to the pressing axis, and also the cooling rate. Especially the demolding force was strongly affected by the cooling rate when the demolding point was located near the glass transition temperature region. These results offer a useful direction for highly accurate glass-molding and glass-imprint processes.

Key words

Imprint; Demolding; Phosphate glass; Borosilicate glass; Young's modulus

1. Introduction

Glass-molding and glass-imprint processes are attractive for the mass manufacturing of several precise optical devices, such as non-spherical or free-form surface lenses, grating, anti-reflection structure, etc. [1-3]. Recently the required geometries become so complicated and highly accurate. Such demands should be never realized unless the rheological behaviors of glass during deformation and demolding are systematically analyzed. One of the serious problems for the glass molding or imprinting process is the fatal damage of glass and/or mold during demolding due to the chemical or physical adhesion of the glass to the mold. Several approaches were reported to reveal the glass molding process such as the numerical simulation for a compression and deformation of glass [4, 5], wettability of molten glass on a heated metal [6, 7], thermal and chemical durability of release film coated on the mold [8-10], surface roughness of mold affecting its adhesion to a glass [11, 12], thermal conductivities of glass and mold [13]. The origins of adhesion between a glass and a mold can be classified into the chemical and the physical interactions. The former means the chemical reactions between the glass and the mold, which are generally caused above the softening temperature of a glass. Almost all of previous studies have been focused on such reactions. On the other hand, there are few studies on the latter.

Even though several new glasses with low softening temperature and new molds with durable release films were developed for the mass

production [3, 14], there is little information on the adhesion of glass to the mold by the physical interaction such as Van der Waals force, which apt to be caused at relatively lower temperature than that due to chemical reaction. Advantageous studies were reported for the polymer-imprint processes [15-17], in where, the maximum tensile force for the separation of a polymer from a mold has been defined as "*demolding force*". It was demonstrated that the demolding force decreased with the Young's moduli of polymers, which were changed by the degree of polymerization [15]. While the compositional dependence of Young's modulus is less sensitive for oxide glasses compared with those for polymers [18], the investigation similar to the concept of polymer-imprint should be possible for the glass-imprint by changing the Young's modulus of molds.

In this study, we focused on the measurement of physical demolding force during the glass-molding or glass-imprint processes. The demolding force was characterized in terms of the tensile force applied to the pressing axis, Young's modulus of mold, and also the cooling rate.

2. Experimental

Commercially available phosphate glass (K-PSK200, Sumita Optical Glass Inc.) and borosilicate glass (L-BAL42, Ohara Inc.) were used in this study. Table 1 shows the properties of these glasses, which were developed for the camera lenses fabricated by the glass-molding process. Flat molds with different Young's modulus were used for the experiment, i.e. a glassy carbon (GC), a SiO_2, and several kinds of tungsten carbides (WC). The properties of molds are summarized in table 2. The Young's moduli of the WC molds were changed by their compositions and sintered grain sizes. The surfaces of SiO_2 and WC molds were coated with 40-nm thick carbon using a rf-sputtering method so as to prevent the chemical reaction between a glass and a mold at high temperature.

Figure 1 shows the set up for the measurement of the deformation and demolding behaviors of glasses. Based on a conventional mold pressing machine, a load cell and a servomotor were set at the lower and upper pressing axes, respectively. A square pit with the area of 10 mm × 10 mm and 1 mm depth was located in the center position on the under a WC mold, in where an optically polished glass plate with 2 mm thickness was placed, consequently the level of top surface of the glass is higher than the mold surface by 1 mm. A flat surface mold of 25 mm × 25 mm × 2 mm for the pressing of a glass was fixed to the upper pressing axis by a WC holder. Therefore, at around the deformation temperature, the glass top surface

contacts with the mold and the glass bottom is tightly supported by the pit during the pressing process, which realizes the monitor of the forces not only for deformation but also for demolding by the load cell. The detection limit of tensile force was 1 MPa for the load cell employed in our set up. The temperatures of upper and lower molds were measured using the thermocouples, which were inserted in each mold. The data transfer rate from the load cell to the storage was 100 points/s. The glass and the mold were heated by a gold image furnace outside the cylindrical silica chamber up to 800°C in a nitrogen atmosphere after the evacuation down to 0.1 Pa in order to inhibit the surface oxidization of molds.

After preheating at the deformation temperature, the glass was pressed by the mold at 2 MPa for 300 s followed by the demolding under a controlled cooling rate by nitrogen gas blowing. Following two kinds of demolding recipes were examined; (a) "*unforced condition*" only by the thermal shrinkage of pressing axes during cooling, (b) "*enforced condition*" by applying an excess tensile force by the servomotor in addition to that due to the axes thermal shrinkage.

3. Results & discussion

3.1. Effect of demolding condition on demolding force

Figure 2 shows a typical measurement result of demolding force for K-PSK200 under the unforced condition. During cooling at the rate of 1ºC /s after the pressing at 2 MPa and 420ºC for 300 s, the load cell detected a tensile force by the adhesion between the glass and the mold, which gradually increased with decreasing the temperature. At a critical maximum, an instantaneous release of the negative force was observed at around 365ºC, which was determined as "*demoling point*" in this study. As shown in figure 2, we defined the maximum tensile force as the "*demolding force"*. Figure 3 shows the demolding forces between the GC mold and K-PSK200 or L-BAL42, obtained under the unforced and enforced conditions: the excess tensile force of 0.5 MPa was applied for the latter case. The glass was deformed by pressing the mold under the pressure of 2 MPa for 300 s at 420ºC for K-PSK200 and 560ºC for L-BAL42, and then cooled at the rate of 1ºC/s to room temperature. It is evident from figure 3 that the demolding forces under the unforced condition are smaller than those under the enforced one. Therefore, we employed the unforced condition for the following experiments, because, actually, no tensile force applied between the mold and the glass in the practical lens manufacturing field.

3.2. Effect of Young's modulus of mold on glass demolding behavior

It was theoretically demonstrated that the adhesion force between contacted two solid surfaces, which means the demolding force in our experiment, depends both on their surface energies and Young's moduli. An adhesion force, F, between the contacted surfaces of two cylindrical elastic solids is described as follows [19];

$$F=(3/2\pi\gamma Ka^3)^{1/2} \quad \cdots (1),$$

$$\gamma=\gamma_1+\gamma_2-\gamma_{12} \quad \cdots (2),$$

$$1/K=3/4[(1-\nu_1^2)/E_1+(1-\nu_2^2)/E_2] \quad \cdots (3),$$

where, $\gamma_{\square\square}$, $\gamma_{\square\square}$ are surface energy of two solids, γ_{12} is interface energy, $\nu_{\square}$, $\nu_{\square}$ and E_1, E_2 are Poisson's ratios and Young's modulus of two solids, respectively, and a is the radius of contact area. From these equations, it is evident that the adhesion force (i.e., the demolding force in our study) should be affected by the Young's modulus. As recognized by the values in table 1, however, there was not so much change in Young's modulus between the different kinds of glasses. Therefore, we used the molds with different Young's modulus for the investigation of demolding behavior. The experimental conditions are identical with those shown in the previous section. Figure 4 shows the relationship between the Young's modulus of molds and the measured demolding force for K-PSK200 and L-BAL42. It is

apparent that the K-PSK200 and L-BAL42 exhibited the similar relationships between the demolding force and the Young's modulus of molds. The lowest force was attained by the GC mold.

Though the mold used for the lens manufacturing requires a high mechanical strength, an adjustment of Young's modulus of the mold should be a solution to prevent the fatal damage of fine patterns fabricated by the glass-imprint.

3.3. Effect of cooling rate on demolding force and demolding point

The tensile force applied to a glass and a mold increased gradually with decreasing the temperature until reaching the demoling point (see figure 2), which means the cooling rate should also be a key factor affecting the demolding force and the demolding point. Thus the difference in the demolding force by changing the cooling rate was investigated. The lowest limit of controllable rate for our set up was 0.1ºC/s. Figure 4 shows demolding forces for K-PSK200 and L-BAL42 with different cooling rate. The K-PSK200 revealed no apparent difference of the force against the cooling rate. Meanwhile, the force for L-BAL42 obviously decreased with increasing the cooling rate. Furthermore, as shown in figure 5, the demolding point increased with the cooling rate both for K-PSK200 and L-BAL42. These tendencies can be explained in terms of the temperature dependence of viscosity. Figure 6 shows the viscosity curves of these glasses measured by the parallel mold method [20, 21]. The solid curves are obtained by the calculation using Vogel-Tamman-Flucher (VTF) equation [22]. The bright and dark gray areas denote the regions of the measured demolding points at the cooling rate of 0.1 and 1.0ºC/s, respectively. It was evident that the demolding points appeared below the glass transition temperature (T_g) without those for L-BAL42 with cooling rate of 1ºC/s, which were crossed over its viscosity curve. In general, there is a drastic change in Young's modulus of a glass around T_g due to its phase transition [23]. Therefore, the

demolding force should be changed sensitively against the cooling rate if the demoling point is located at around T_g. The demolding points for K-PSK200 were always appeared far lower than the T_g, consequently exhibiting no dependence of demolding force against the cooling rate. Further systematic investigation for several kinds of glasses is required for the elucidation of complicated viscoelastic behaviors of glass during demolding process, which will certainly give valuable principles not only for glass-molding but also glass-imprinting.

4. Conclusion

The demolding behaviors were investigated quantitatively for oxide glasses under the condition where no chemical reaction occurs between glass and mold. The demolding force decreased with the tensile force applied to the mold. There were clear relationships between the Young's modulus of mold and the demolding force. In order to minimize the demolding force, a lower Young's modulus of the mold is preferred if its life time and forming accuracy are tolerated. Furthermore, a rapid cooling increased the demolding point, hence, decreasing the demolding force if the demolding point was located near the glass transition temperature region. Hence, the Young's modulus of mold and cooling rate are important factors for a glass molding and a glass-imprint to fabricate highly accurate optical components.

5. Acknowledgment

We would like to thank FUJI DIE CO., LTD for providing WC molds.

6. References

[1] T. Tamura, M. Umetani, K. Yamada, Y. Tanaka, K. Kintaka, H. Kasa, J. Nishii, Fabrication of antireflective subwavelength structure on spherical glass surface using imprinting process, Appl. Phys. Exp., 3 (2010) 112501.

[2] T. Mori, K. Hasegawa, T. Hatano, H. Kasa, K. Kintaka, J. Nishii, Surface-relief gratings with high spatial frequency fabricated using direct glass imprinting process, Opt. Lett., 33 (2008) 428-430.

[3] H. Takebe, M. Kuwabara, M. Komori, N. Fukugami, M. Soma, T. Kusuura, Imprinted optical pattern of low-softening phosphate glass, Opt. Lett., 32 (2007) 2750-2752.

[4] C. Druma, M.K. Alam, A.M. Druma, A. Hoque, Finite element analysis of TV panel glass during cooling, Mater. Manuf. Processes, 19 (2004) 1171-1187.

[5] A. Jain, A.Y. Yi, Numerical modeling of viscoelastic stress relaxation during glass lens forming process, J. Am. Ceram. Soc., 88 (2005) 530-535

[6] D. Zhong, E. Mateeva, I. Dahan, J.J. Moore, G.G.W. Mustoe, T. Ohno, J. Disam, S. Thiel, Wettability of NiAl, Ni-Al-N, Ti-B-C, and Ti-B-C-N films by glass at high temperatures, Surf. Coat. Technol., 133 (2000) 8-14.

[7] J. Pech, M. Braccini, A. Mortensen, N. Eustathopoulos, Wetting, interfacial interactions and sticking in glass/steel systems, Mater. Sci. Eng., A 384 (2004) 117-128.

[8] A.P. Tomsia, Z. Feipeng, J.A. Pask, Reactions and bonding of sodium disilicate glass with chromium, J. Am. Ceram. Soc., 68 (1985) 20-24.

[9] P. Manns, W. Doll, G. Kleer, Glass in contact with mould materials for container production, Glass Sci. Technol., 68 (1995) 389-399.

[10] R.C. Dartnell, H.V. Fairbanks, W.A. Koehler, Investigation of the

adherence of glass to metals and alloys, J. Am. Ceram. Soc., 34 (1951) 357-360.

[11] J. Pech, G. Berthome, M. Jeymond, N. Eustathopoulos, Influence of glass/mould interfaces on sticking, Glass Sci. Technol., 78 (2005) 54-62.

[12] K.D. Fischbach, K. Georgiadis, F. Wang, O. Dambon, F. Klocke, Y. Chen, A.Y. Yi, Investigation of the effects of process parameters on the glass-to-mold sticking force during precision glass molding, Surf. Coat. Technol., 205 (2010) 312-319.

[13] W. Hiroshi, S. Isao, Mechanism dominating the generation of sink-Mark and residual stress in a press-formed glassware from a thermal engineering viewpoint, Trans. Jpn. Soc. Mech. Eng., B 68 (2002) 1181-1189.

[14] D. Rieser, G. Spiess, P. Manns, Investigations on glass-to-mold sticking in the hot forming process, J. Non-Cryst. Solids, 354 (2008) 1393-1397.

[15] A. Amirsadeghi, J.J. Lee, S. Park, Surface adhesion and demolding force dependence on resist composition in ultraviolet nanoimprint lithography, Appl. Surf. Sci., 258 (2011) 1272-1278.

[16] H. Kawata, Y. Watanabe, N. Fujikawa, M. Yasuda, Y. Hirai, Impact of substrate deformation on demolding force for thermal imprint process, J. Vac. Sci. Technol., B 28 (2010) C6M77-82.

[17] V. Trabadelo, H. Schift, S. Merino, S. Bellini, J. Gobrecht, Measurement of demolding forces in full wafer thermal nanoimprint, Microelectron. Eng., 85 (2008) 907-909.

[18] S. Inaba, S. Fujino, K. Morinaga, Young's modulus and compositional parameters of oxide glasses, J. Am. Ceram. Soc., 82 (1999) 3501-3507.

[19] H.M. Pollock, D. Maugis, M. Barquins, Force of adhesion between solid-surfaces in contact, Appl. Phys. Lett., 33 (1978) 798-799.

[20] A.N. Gent, Theory of the parallel plate viscometer, Br. J. Appl. Phy., 11

(1960) 85-87.

[21] E.H. Fontana, A versatile parallel-plate viscometer for glass viscosity measurements to 1000 degrees C, Am. Ceram. Soc. Bull., 49 (1970) 594-597.

[22] C.A. Angell, Relaxation in liquids, polymers and plastic crystals - strong fragile patterns and problems, J. Non-Cryst. Solids, 131 (1991) 13-31.

[23] L. Duffrene, R. Gy, J.E. Masnik, J. Kieffer, J.D. Bass, Temperature dependence of the high-frequency viscoelastic behavior of a soda-lime-silica glass, J. Am. Ceram. Soc., 81 (1998) 1278-1284.

7. Figures

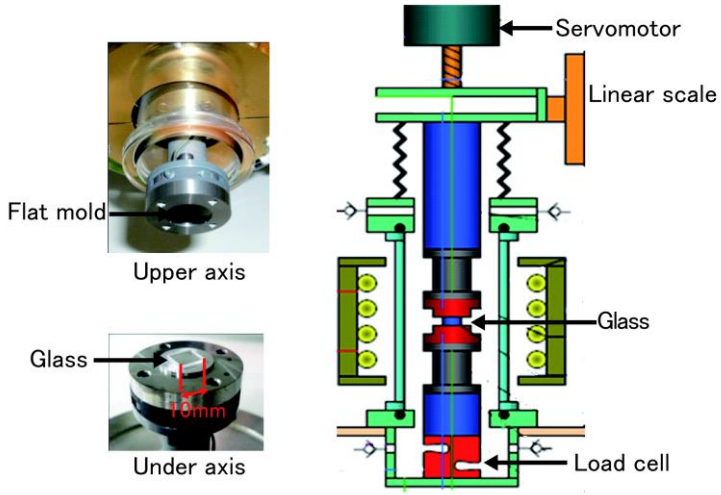

Figure 1. Diagram of the glass molding machine for evaluations of demoling force and demolding point.

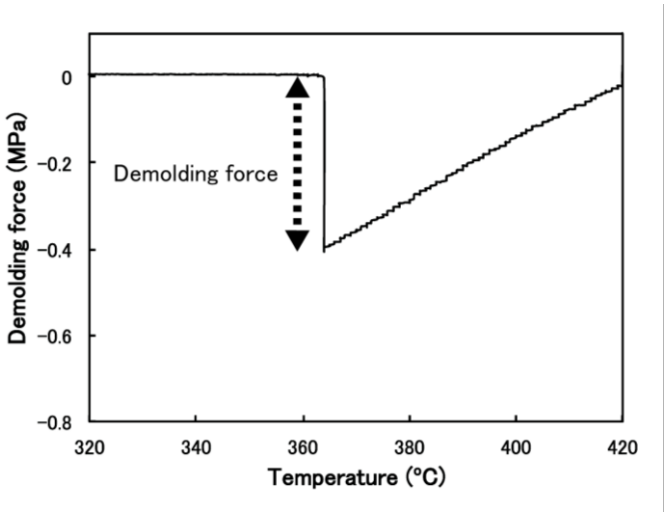

Figure 2. Typical measurement data of demolding force obtained under the unforced demolding condition for K-PSK200 pressed by the GC mold at 2 MPa and 420ºC for 300 s, and cooled at the rate of 1 ºC/s.

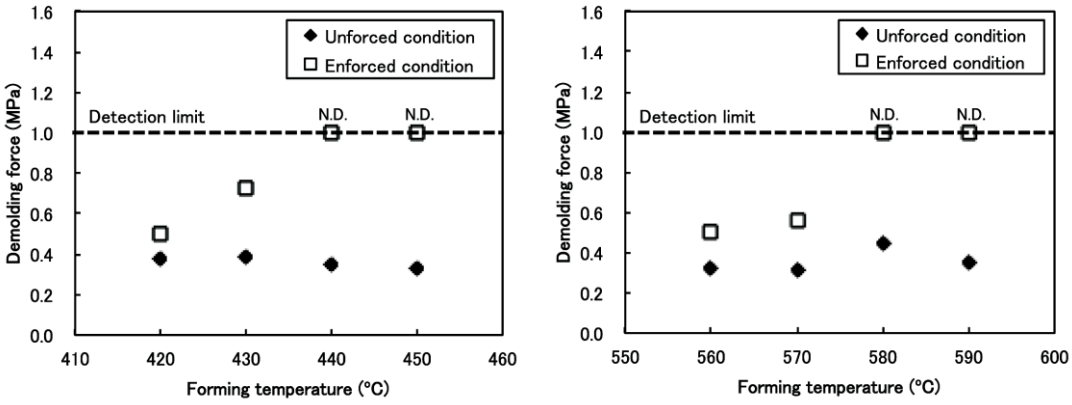

Figure 3. Demolding forces measured for (a) K-PSK200 and (b) L-BAL42 under unforced demolding and enforced demolding conditions after the pressing at 2 MPa using the GC mold with 2 mm thickness and various temperatures for 300 s. The tensile force of 0.5 MPa was applied for the enforced demolding condition. Upper detection limit of demolding force was 1 MPa, which was decided by the specification of load cell.

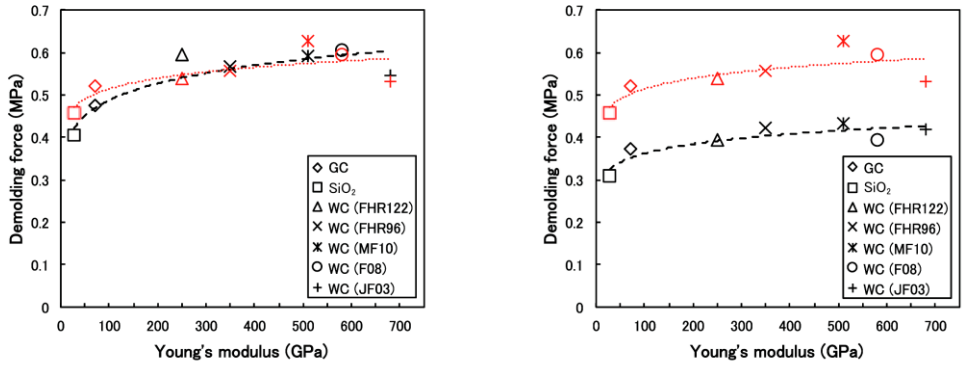

Figure 4. Effects of Young's modulus of molds and cooling rate on demolding force. The glasses were pressed at 2 MPa for 300 s using various molds with 2 mm thickness listed in table 2. The pressing temperatures were 420ºC for (a) K-PSK200 and 560ºC for (b) L-BAL42, respectively. The glasses were cooled at the rate of 0.1ºC/s (red symbol and dot line) or 1ºC/s (black symbol and dash line).

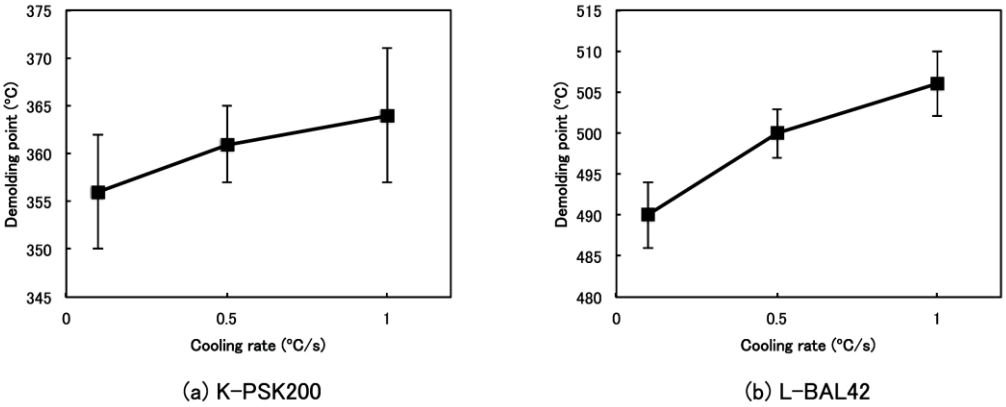

Figure 5. Relationships between cooling rate and demolding point for (a) K-PSK200 and (b) L-BAL42 after pressing at 2 MPa for 300 s using the GC mold. The pressing temperature was 420ºC for K-PSK200 and 560ºC for L-BAL42, respectively.

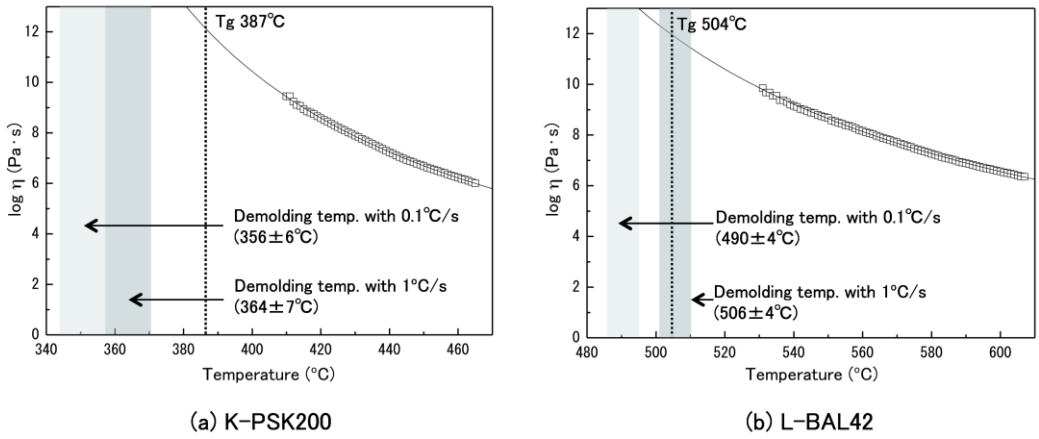

Figure 6. Temperature dependences of viscosities for (a) K-PSK200 and (b) L-BAL42, which were measured by a parallel plate method (opened square symbol) and fitted by the VTF equation (solid line). Bright and dark gray zones denote the temperature regions where the demolding points appeared by the cooling at the rate of 0.1 and 1 ºC/s, respectively.

8. Tables

Table 1. Thermal and physical properties of glasses used in this study.

Glass	T_g (ºC)	Thermal conductivity ($Wm^{-1}k^{-1}$)	Thermal expansion coefficient ($\times 10^{-7}$ ºC^{-1})	Young's modulus (GPa)
Phosphate glass (K-PSK200, Sumita Optical Glass, Inc.)	387	0.7	123	72
Borosilicate glass (L-BAL42, Ohara Inc.)	504	1.0	88	89

Table 2. Thermal and physical properties of molds used in this study.

Mold	Surface roughness, Ra (nm)	Thermal conductivity ($Wm^{-1}k^{-1}$)	Thermal expansion coefficient ($\times 10^{-7}$ ºC^{-1})	Young's modulus (GPa)
GC	1.3	6	20	27
SiO_2	2.5	2	5	72
WC (FHR122)	14.0	62	58	250
WC (FHR96)	11.2	54	55	350
WC (MF10)	2.1	29	61	510
WC (F08)	1.4	29	57	560
WC (JF03)	3.1	62	45	680